

Cite this: *Chem. Sci.*, 2023, 14, 14256

All publication charges for this article have been paid for by the Royal Society of Chemistry

Received 27th September 2023

Accepted 16th November 2023

DOI: 10.1039/d3sc05071h

rsc.li/chemical-science

Rapid, iterative syntheses of unsymmetrical di- and triarylborananes from crystalline aryldifluoroborananes†

Douglas Turnbull and Marc-André Légaré *

A one-pot procedure to synthesise aryldifluoroborananes, ArBF_2 , from bench-stable arylsilanes is presented. These ArBF_2 react conveniently with aryllithium reagents to form unsymmetrical $\text{ArAr}'\text{BF}$ and $\text{BARAr}'\text{Ar}''$ in high yield. Examples of all three classes of borane have been characterised crystallographically, allowing for elucidation of geometric and crystal packing trends in crystalline ArBF_2 .

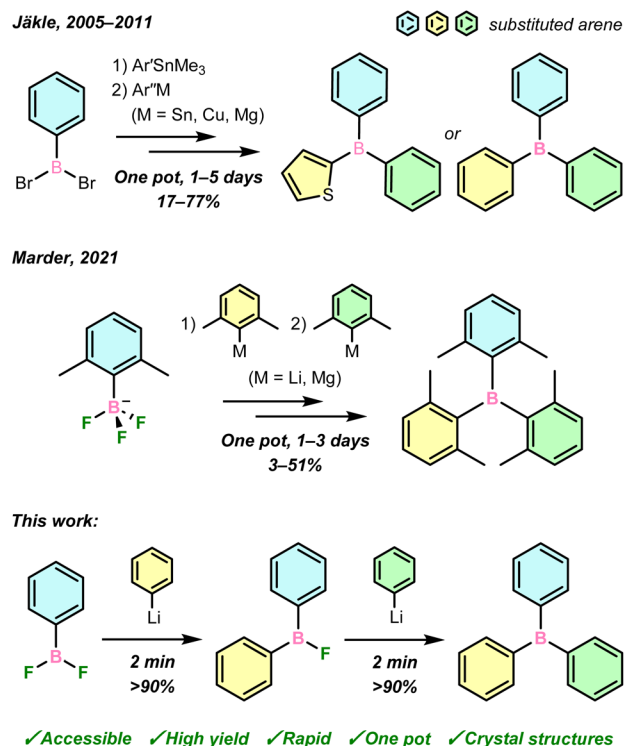
Introduction

Triarylborananes, bolstered by over a century of continuous research, find importance across chemical disciplines such as in metal-free catalysis,^{1,2} anion sensing,³ optoelectronic materials,⁴ and cell imaging.⁵ Their uniquely advantageous properties are governed, in part, by the electron deficiency of the central boron atom, whose unoccupied p orbital can both mediate reactivity and be part of an extended conjugated π -system as an electron acceptor.

Equally important is the nature of the aryl groups, which must be tailored to fine-tune the desired steric and electronic properties of triarylborananes, such as their Lewis acidity, solubility in aqueous and/or organic media, and kinetic stability to hydrolysis. As was recently highlighted by Marder and co-workers in an extensive synthetic review,⁶ numerous methods have been reported to synthesise triarylborananes by substitution reactions of aryl nucleophiles with commercial BX_3 ($\text{X} = \text{H}, \text{OR}, \text{F}, \text{Cl}, \text{Br}$) sources. However, such substitutions overwhelmingly produce symmetrically substituted BAR_3 or $\text{BAR}_2\text{Ar}'$ ($\text{Ar} = \text{aryl}$) due to the presence of several complex equilibria,⁷ the importance of each being governed by the natures of the BX_3 source, nucleophile, and extrinsic conditions. This inherently limits reaction control, and consequently the potential diversity, and thus applications, of the resultant boranes.

Further diversification to fully unsymmetrical $\text{BARAr}'\text{Ar}''$, meanwhile, has hitherto proven to be a significant contemporary synthetic challenge, thereby limiting modern advances in our understanding and application of boron-containing compounds. A small number of $\text{BARAr}'\text{Ar}''$ have been prepared using M/B ($\text{M} = \text{Li}, \text{MgBr}$) exchange with ArBX_2 ($\text{X} = \text{H},^8 \text{Br},^9 \text{OR}^{10}$), or Pd-

catalysed cross-coupling to symmetric boranes,^{11–14} usually requiring multi-step protocols. These studies have demonstrated the possible applications of $\text{BARAr}'\text{Ar}''$ in fluorescence imaging and small-molecule sensing for biological systems, though their synthetic routes were target-specific, rather than general. Jäkle and co-workers first approached a more iterative $\text{BARAr}'\text{Ar}''$ synthesis *via* $\text{Me}_3\text{Sn/B}$ exchange with ArBBr_2 , followed by transmetalation with aryl-magnesium, -copper, or -tin reagents (Scheme 1, top).^{15–19} However, the toxicity of Me_3Sn and ArCu reagents is a drawback to such an approach. Only recently,



Scheme 1 Iterative approaches to triarylborane synthesis.

Department of Chemistry, McGill University, Otto Maass Chemistry Building, 801 Rue Sherbrooke O, Montreal, Quebec, Canada H3A 0B8. E-mail: ma.legare@mcgill.ca

† Electronic supplementary information (ESI) available. CCDC 2292569–2292582 and 2305672. For ESI and crystallographic data in CIF or other electronic format see DOI: <https://doi.org/10.1039/d3sc05071h>

Marder and co-workers reported the stepwise transmetallation of $K[ArBF_3]$ complexes with 2,6-disubstituted aryllithium or Grignard reagents to generate triarylborananes (Scheme 1, middle).²⁰ In both this and the Sn-mediated cases, reactions can take days with poor-to-moderate overall yields.

In light of the promising properties of triarylborananes highlighted above, iterative syntheses of $BARAr'Ar''$ through stepwise arylation of a reactive boron centre represents an attractive avenue for development of new boron-containing molecules and materials. An ideal synthetic approach for the preparation of diverse triarylborananes would be capable of selectively substituting accessible boron sources rapidly and in high yields, using convenient aryl nucleophiles. This would improve both the simplicity and scope of modern borane synthesis, and notably enable the synthesis of $BARAr'Ar''$ in which each aryl substituent possesses uniquely tailored, application-driven steric and electronic properties.

Herein, we demonstrate that crystalline $ArBF_2$ are easily accessed from air-stable silanes in a one-pot protocol, which has allowed for their multigram-scale isolation and their use as privileged reagents in organometallic boron chemistry. Specifically, they react conveniently with aryllithium reagents in rapid and selective transmetallations to form unsymmetrical $ArAr'BF$ and $BARAr'Ar''$ in one pot, in high yield and within minutes, from which LiF is the sole by-product (Scheme 1, bottom). These boranes have been comprehensively characterised in the solid state and in solution, including the first crystal structures of unsymmetrical $ArAr'BF$.

Results and discussion

Syntheses of aryl difluoroborananes (3)

Our synthetic route was developed from a previous reaction of $PhBCl_2$ with main-group fluoroanions, which gave $PhBF_2$ in >95% yield after vacuum distillation.²¹ We have instead proceeded *via* reaction of bench-stable $ArSiMe_2R$ (**1**, $R = Me$ except for **1b**, where $R = H$) with BBr_3 in CH_2Cl_2 to form $ArBBr_2$ (**2**) *in situ* followed by solvent removal and direct addition of $Na[BF_4]$ (Scheme 2). The desired $ArBF_2$, **3**, are formed in moderate-to-high isolated yields and high purity but can be further purified by vacuum sublimation and/or recrystallisation. These conditions tolerate arenes with steric hindrance (**3a–b**), polycyclic aromatic systems (**3c–e**), multiple boryl substituents (**3f–g**), and heteroatoms (**3h**).

Isolated **3** are typically colourless, crystalline solids that sublime readily upon heating or *in vacuo*, including **3a**, which was previously reported to be a colourless liquid.²² In all cases, they are highly soluble in common organic solvents and easily handled using standard glove box techniques. Exposure to moisture, however, results in fuming and formation of $[ArBO]_3$, ArH , and BF_3 as hydrolysis products, determined by NMR spectroscopy.

Boron tribromide was preferred for the Si/B exchange step due to greater reactivity towards $ArSiMe_3$ than BCl_3 and demonstrated reactivity with sterically demanding silanes, *e.g.*, **1a**.²³ Reactions were performed with dimethylsilane **1b** due to the steric hindrance of the C_6Me_5 group preventing preparation



Scheme 2 Isolated yields (unless noted otherwise) from one-pot syntheses of aryl difluoroborananes (**3**) *via* stepwise Si/B and Br/F exchange of arylsilanes (**1**). [a] Reaction of **1b** with BBr_3 (3.0 eq.) was run for 2 h. [b] Prepared directly from **2f**. [c] Reaction of **1g** with BBr_3 was run for 3 h at 70 °C in 1,2-dichloroethane. [d] Prepared using 8.0 equiv. $Na[BF_4]$.

of the corresponding trimethylsilane. This increased bulk slowed the Si/B exchange step, with incomplete conversion revealing intermediate Si–H bromination. Electron-deficient arenes were previously found not to undergo the necessary Si/B exchange,²⁴ and we have found that $ArNMe_2$ derivatives are also incompatible due to the formation of inert BBr_3 adducts (Fig. S1†).

No $[ArBF_3]^-$ was observed even when using excess $Na[BF_4]$, indicating the weaker Lewis acidity of **3** than BF_3 , which is supported by F^- exchange energy calculations (Table S1†) and a previous NMR study of related $ArBF_2$.²⁵ Our route thus complements a recent synthesis of $[ArBF_3]^-$ reported by Perrin and co-workers using an ostensibly similar metathesis of $ArB(OH)_2$ with $[BF_4]^-$ in alcoholic solvents.²⁶

Spectroscopic and crystallographic studies of 3

Consistent with previously reported NMR spectra,²⁷ the ^{11}B NMR spectra of **3** (C_6D_6 , 298 K) give rise to broad triplets at approximately 25 ppm ($^1J_{BF}$ *ca.* 75 Hz), whereas the ^{19}F NMR spectra give rise to pseudo-doublets (quadrupole-collapsed equal-intensity quartets) between *ca.* –57 and –90 ppm. The ^{11}B and ^{19}F chemical shifts calculated for **3** in C_6H_6 using DFT agree well with the experimental values (Table S2†).

The crystal structures of **3** at 150 K (Fig. 1, top), refined to high accuracy using non-spherical atomic scattering factors (see the ESI†), reveal B–F bonds shorter than in BF_3 (in Å, 1.26–1.31),²⁸ similar to previously reported $ArBF_2$ (1.307(2)–



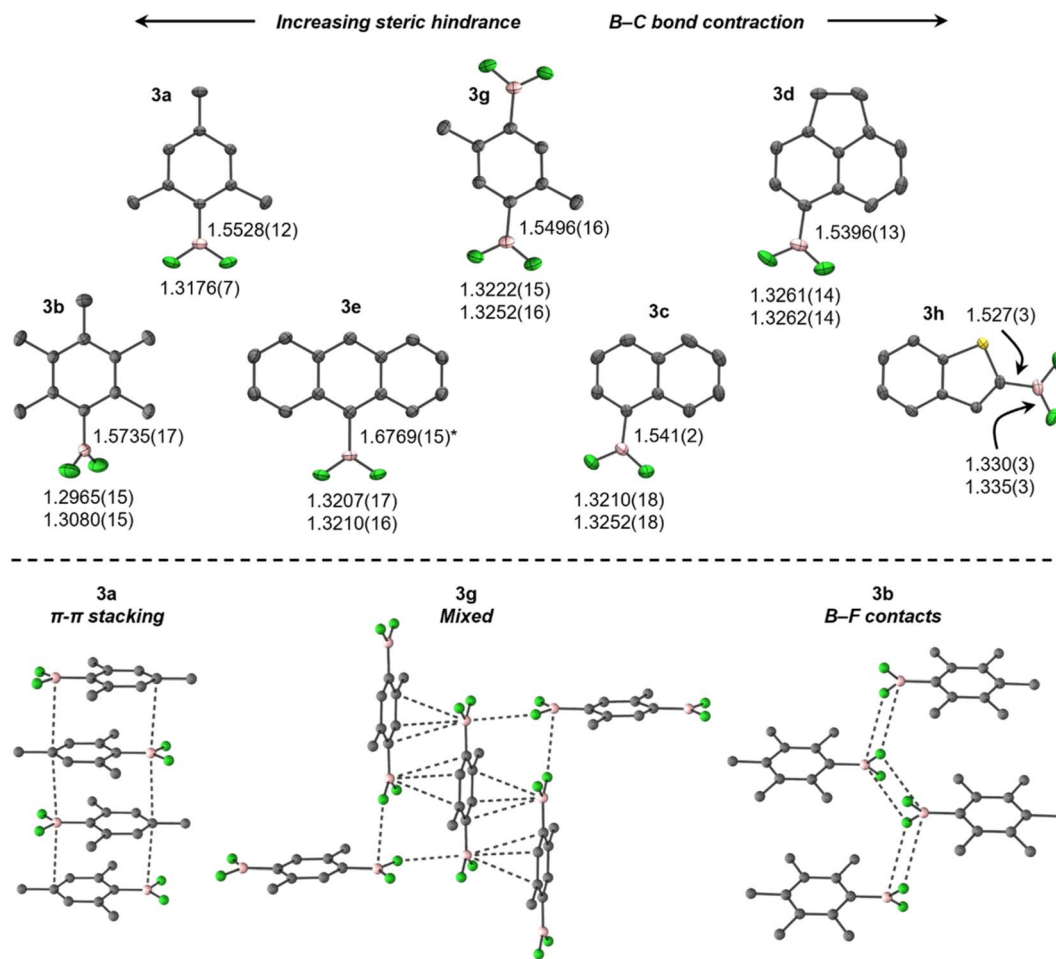


Fig. 1 Top: Thermal ellipsoid plots (50% probability level) of aryldifluoroboranes (**3**), with B-C and B-F bond lengths (in Å). Colours denote F (green), B (pink), and C (grey), with H atoms omitted for clarity. Asterisk (*) denotes an artificially elongated B-C bond due to 50/50 H/BF₂ disorder. Bottom: Selected crystal packing diagrams for **3**.

1.3146(15)),^{29,30} B-BF₂ (1.24(3)–1.359(5)),^{31–34} and Pt-BF₂ (1.324(7)–1.344(4))^{32,35–37} systems, but contracted in comparison to [ArBF₃][−], e.g., [N(^{*n*}Bu)₄][PhBF₃] (1.409(3)–1.426(2)).³⁸ When ordered in terms of steric bulk, the B-F bonds elongate only subtly from **3h** (least hindered) to **3a** (most), but are significantly shorter in **3b**, comparably to EindBF₂ and TerBF₂.^{29,30} In contrast, a more conspicuous contraction of the B-C bond occurs with increasing bulk in **3**. These trends are attributed to, at least in part, steric pressure caused by crystal packing (*vide infra*), as no obvious trends in geometric parameters were observed in solution-phase optimised geometries (Table S3†), which otherwise agree well with the experimental data.

The crystal structures of **3** exhibit diverse solid-state interactions (Fig. 1, bottom). Their planarity facilitates π - π stacking wherein the BF₂ moieties are situated over comparatively electron-rich aryl rings in adjacent molecules, except for **3b**, which is non-planar ($\tau(\text{F1-B-C1-C2}) = 60.58(15)^\circ$) and prefers fluorine layers containing zig-zag chains of B-F contacts. Interestingly, **3g** and **3h** adopt B-F contacts at only one face of the boron atom, which is flanked by a π - π stacking/B-S interaction (Fig. 2). The contacts are weaker in **3b** (in Å, 3.326), **3g** (3.070) and

3h (3.210) than BF₃ (2.68–2.71),²⁸ but still within the sum of van der Waals radii (3.39).³⁹ In contrast, steric crowding in EindBF₂ and TerBF₂ prevents any notable contacts to boron.^{29,30}

The large difference in torsion angle and packing motif between **3a** and **3b** is notable, given that they differ only by the presence of *meta*-methyl groups in **3b**. The C₁-C₆-C_{Me} angle in **3a** (123.02(6)°) suggests a slight repulsion of the *ortho*-methyl groups from the BF₂ moiety to facilitate planarity, but this is seemingly blocked in **3b** (120.36(11), 120.60(11)°) and thus torsion occurs. This is attributed to a resonance effect from boron in **3a**, rather than crystal packing, as it is reflected in the optimised geometries (123.04, 123.14° in **3a** vs. 120.67, 120.76° in **3b**). The planarity and presence of π - π stacking in **3a** may also rationalise its crystallinity *versus* heavier MesBX₂, which are minimally volatile liquids at ambient temperature.^{40,41} This is supported by calculated solution-phase **3a**/MesBX₂ head-to-tail dimers, which show considerable disruption of stacking by twisting of the larger BX₂ moieties out of plane (Fig. S3†). The enthalpies and Gibbs energies reflect this, being most exothermic and least endergonic for **3a** (Fig. S3†).



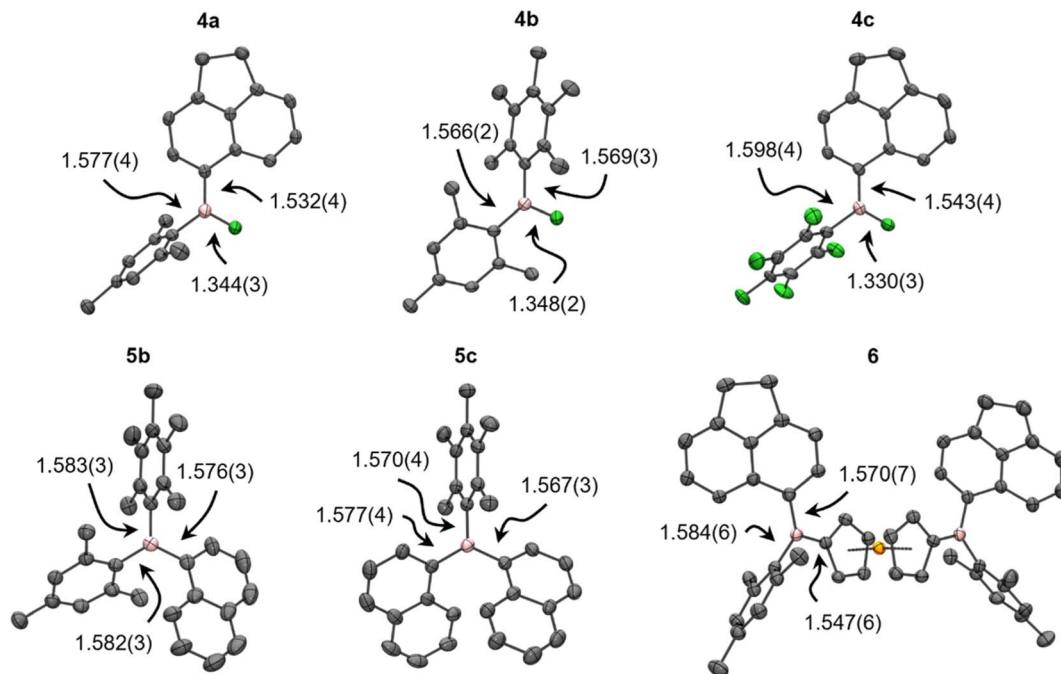


Fig. 2 Thermal ellipsoid plots of diaryl- (**4**, 150 K, 50% probability level) and triarylboranes (**5b**, **5c** and **6**, 298 K, 20% probability level), with B–C and B–F bond lengths (in Å). Colours denote Fe (orange), F (green), B (pink), and C (grey), with H atoms omitted for clarity.

Syntheses of di- (**4**) and triarylboranes (**5/6**)

To establish the utility of **3** in organoboron chemistry, derivatisation with aryl nucleophiles was performed (Scheme 3). Stoichiometric reactions with simple, moderately sterically shielded aryllithium or Grignard reagents, *i.e.*, MesLi and C_6F_5MgBr , were found to selectively produce unsymmetrical $ArAr'BF$ (**4a–d**) in quantitative yield after *ca.* 2 min at ambient temperature. These could be isolated in high yield after recrystallisation or derivatised in one pot to unsymmetrical naphthyl- (**5a**, **5b**) and ferrocenyl-substituted (**6**) boranes with the respective aryllithium reagent in similarly rapid conversion and high yield. The generation of less hindered $ArAr'BF$ using **3d** shows that steric freedom in **3** does not negatively impact selectivity upon transmetallation under these circumstances. Furthermore, the convenient generation of unsymmetrical C_6F_5 -substituted boron using C_6F_5MgBr in Et_2O is especially notable considering the importance of electron-withdrawing groups in boron chemistry. By contrast, typical approaches have used C_6F_5Cu and introduced C_6F_5 as a final step.²⁷ Overall, these reactions demonstrate that **4** are versatile precursors that, for the first time, allow for direct access to unsymmetrical boranes within minutes.

Reactions of **3** with less hindered NaphLi and Ar^FMgBr ($Ar^F = 3,5-(CF_3)_2C_6H_3$) were found to result in distributions of the desired $ArAr'BF$, symmetrical $BAr(Ar')_2$, and unreacted **3**, and were investigated by NMR spectroscopy (Table S1†). Under typical conditions, *i.e.*, in Et_2O at ambient temperature, **3b** and NaphLi afforded the desired $ArAr'BF$ in only *ca.* 10% NMR yield, though symmetrical $BAr(Ar')_2$ **5c** was generated quantitatively with 2 equiv. of NaphLi. This yield increased to *ca.* 40 and 60%

in benzene and pentane, respectively, though cooling the reaction in pentane to $-35\text{ }^\circ\text{C}$ had no effect on yield. The steric profile of **3** also began to influence product distribution, as **3a** and **3d** afforded the corresponding $ArAr'BF$ in 40 and 10% yields upon reaction with NaphLi in pentane. Notably, the use of electron withdrawing Ar^FMgBr significantly improved selectivity, as reactions of **3a** with Ar^FMgBr in Et_2O afforded $ArAr'BF$ in 70% yield despite the more polar solvent and absence of *ortho*-substitution. In contrast, bulky dibromoborane **2b** showed no selectivity during transmetallation with MesLi or NaphLi.

These findings highlight the specific utility of fluoroboranes in transmetallations with aryllithium and Grignard reagents. We attribute this to the high electrophilicity of boron improving the rate of B–C bond formation, while the strength of the B–F bond mitigates F^- dissociation and subsequent overreaction.⁸ The observed effects of solvent, sterics of the borane and aryl nucleophile, and electronics of the nucleophile, on selectivity serve as complements to previous observations on solvent and electronic effects in reactions of $B(OR)_3$ ($R = \text{alkyl}$) with Grignard reagents.⁸

Spectroscopic and crystallographic studies of **4–6**

The asymmetry of **4–6** was established by complete assignment of the multi-nuclear NMR spectra (see the ESI†). The transformations of **3** to **4**, and then **4** to **5/6**, were easily monitored by ^{11}B and ^{19}F NMR spectroscopy, the former revealing high-frequency shifts to *ca.* 50, then 75 ppm, and the later showing shifts to >-40 ppm before disappearing entirely. The calculated ^{11}B chemical shifts of **4–6** agree well with experimental data,





Scheme 3 Isolated yields of transmetalations with aryldifluoroboranes (**3**) to form di- (**4**) and triaryldifluoroboranes (**5–7**). [a] Reaction was run in pentane at $-35\text{ }^{\circ}\text{C}$.

though the ^{19}F resonances of the B–F moiety in **4** are systematically overestimated to varying extents (≤ 20 ppm), which is attributed to dynamic aryl ring rotation not being captured in the static shielding tensor calculations.

In addition to NMR spectroscopy, the asymmetry of **4–6** was confirmed, where possible, using X-ray crystallography (Fig. 2, Table S5[†]); to our knowledge, the crystal structures of **4a–c** are the first to be reported for unsymmetrical $\text{ArAr}'\text{BF}$. The B–F bonds are significantly longer than in **3**, more comparable to symmetric Ar_2BF (1.312(3)–1.354(2) Å).^{15,29,42–44} The B–C bonds are, however, insignificantly different from their counterparts in **3**. The trigonal plane at boron is coplanar with the less sterically hindered aryl group and the increased steric shielding prevents any notable solid-state contacts to boron. Meanwhile, increased strain in **5b**, **5c** results in B–C bonds elongated to a similar extent as in, e.g., BMe_3 (1.58 Å).⁴⁵ Likewise, the B–C bonds in **6** reflect those observed in unsymmetrical 1-borylferrocenes (1.546(5)–1.553(3) Å for B–C(Fe), 1.567(6)–1.585(5) Å otherwise).¹⁶

Conclusions

In conclusion, we have developed a facile and general synthetic route to solid aryldifluoroboranes, allowing for their crystallographic study. This has revealed subtle trends in solid-state geometric parameters as a function of the steric demands of the aryl group, as well as the diversity of their crystal packing motifs. Furthermore, they are shown to react selectively with aryllithium reagents to form unsymmetrical di- and triaryldifluoroboranes within minutes, with a selectivity that arises from steric and electronic factors. Thus, aryldifluoroboranes may provide an accessible avenue for modular borane synthesis with broad potential application in organoboron chemistry; investigations into further preparation and functionalisation of such unsymmetrical species are currently underway.

Data availability

The data that supports the findings of this article are included in the ESI.[†]

Author contributions

Experiments and computations were designed and performed by D. T. Data analysis and manuscript preparation were performed by D. T. The project was overseen by M.-A. L.

Conflicts of interest

There are no conflicts to declare.

Acknowledgements

We would like to thank Alexander S. Wahba for high-resolution mass-spectrometric analysis, Prof. Scott Bohle for access to his Bruker Apex II diffractometer, along with Thierry Maris and Daniel Chartrand at l'g Université de Montréal for access to their Bruker Metaljet X-ray diffractometer. We also thank the Natural Sciences and Engineering Research Council of Canada (NSERC) for a Discovery Grant (M.-A. L.; RGPIN-2021-03814) and Postdoctoral Fellowship (D. T.), as well as McGill University, the Canada Foundation for Innovation (CFI), and the Digital Research Alliance of Canada for funding and resources.

Notes and references

- J. L. Carden, A. Dasgupta and R. L. Melen, *Chem. Soc. Rev.*, 2020, **49**, 1706–1725.
- V. Nori, F. Pesciaoli, A. Sinibaldi, G. Giorgianni and A. Carlone, *Catalysts*, 2022, **12**, 5.
- H. Zhao, L. A. Leamer and F. P. Gabbaï, *Dalton Trans.*, 2013, **42**, 8164–8178.
- S. K. Mellerup and S. Wang, *Trends Chem.*, 2019, **1**, 77–89.
- S. M. Berger and T. B. Marder, *Mater. Horiz.*, 2022, **9**, 112–120.
- S. M. Berger, M. Ferger and T. B. Marder, *Chem.–Eur. J.*, 2021, **27**, 7043–7058.



- 7 T. Klis, A. Libura and J. Serwatowski, *Main Group Met. Chem.*, 2002, **25**, 479–484.
- 8 R. J. Blagg and G. G. Wildgoose, *RSC Adv.*, 2016, **6**, 42421–42427.
- 9 M. J. Kelly, R. Tirfoin, J. Gilbert and S. Aldridge, *J. Organomet. Chem.*, 2014, **769**, 11–16.
- 10 M. Ito, E. Ito, M. Hirai and S. Yamaguchi, *J. Org. Chem.*, 2018, **83**, 8449–8456.
- 11 J. Liu, S. Zhang, C. Zhang, J. Dong, C. Shen, J. Zhu, H. Xu, M. Fu, G. Yang and X. Zhang, *Chem. Commun.*, 2017, **53**, 11476–11479.
- 12 J. Liu, C. Zhang, J. Dong, J. Zhu, C. Shen, G. Yang and X. Zhang, *New J. Chem.*, 2017, **41**, 4733–4737.
- 13 J. Liu, C. Zhang, J. Dong, J. Zhu, C. Shen, G. Yang and X. Zhang, *RSC Adv.*, 2017, **7**, 14511–14515.
- 14 X. Yin, K. Liu, Y. Ren, R. A. Lalancette, Y.-L. Loo and F. Jäkle, *Chem. Sci.*, 2017, **8**, 5497–5505.
- 15 S. M. Cornet, K. B. Dillon, C. D. Entwistle, M. A. Fox, A. E. Goeta, H. P. Goodwin, T. B. Marder and A. L. Thompson, *Dalton Trans.*, 2003, 4395–4405.
- 16 H. Li, A. Sundararaman, T. Pakkirisamy, K. Venkatasubbaiah, F. Schödel and F. Jäkle, *Macromolecules*, 2011, **44**, 95–103.
- 17 A. Sundararaman, M. Victor, R. Varughese and F. Jäkle, *J. Am. Chem. Soc.*, 2005, **127**(40), 13748–13749.
- 18 K. Parab, K. Venkatasubbaiah and F. Jäkle, *J. Am. Chem. Soc.*, 2006, **128**(39), 12879–12885.
- 19 K. Parab, A. Doshi, F. Cheng and F. Jäkle, *Macromol.*, 2011, **44**(15), 5961–5967.
- 20 M. Ferger, S. M. Berger, F. Rauch, M. Schönitz, J. Rühle, J. Krebs, A. Friedrich and T. B. Marder, *Chem. Eur.-J.*, 2021, **27**(35), 9094–9101.
- 21 O. Farooq, *J. Fluorine Chem.*, 1995, **70**, 225–227.
- 22 G. Bir, W. Schacht and D. Kaufmann, *J. Organomet. Chem.*, 1988, **340**, 267–271.
- 23 D. Kaufmann, *Chem. Ber.*, 1987, **120**, 853–854.
- 24 H.-J. Frohn, H. Franke, P. Fritzen and V. V. Bardin, *J. Organomet. Chem.*, 2000, **598**, 127–135.
- 25 M. M. Shmakov, S. A. Prikhod'ko, R. Y. Peshkov, V. V. Bardin and N. Y. Adonin, *Mol. Catal.*, 2022, **521**, 112202.
- 26 J. Lozada, W. Xuan Lin, R. M. Cao-Shen, R. Astoria Tai and D. M. Perrin, *Angew. Chem., Int. Ed.*, 2023, **62**, e202215371.
- 27 A. Sundararaman, K. Venkatasubbaiah, M. Victor, L. N. Zakharov, A. L. Rheingold and F. Jäkle, *J. Am. Chem. Soc.*, 2006, **128**, 16554–16565.
- 28 D. Mootz and M. Steffen, *Angew. Chem., Int. Ed. Engl.*, 1980, **19**, 483–484.
- 29 D. Duvinage, L. A. Malaspina, S. Grabowsky, S. Mebs and J. Beckmann, *Eur. J. Inorg. Chem.*, 2023, **26**, e202200482.
- 30 T. Murotsuki, S. Kaneda, R. Maruhashi, K. Sadamori, Y. Shoji, K. Tamao, D. Hashizume, N. Hayakawa and T. Matsuo, *Organometallics*, 2016, **35**, 3397–3405.
- 31 J. C. Jeffery, N. C. Norman, J. A. J. Pardoe and P. L. Timms, *Chem. Commun.*, 2000, 2367–2368.
- 32 J. H. Muessig, D. Prieschl, A. Deisenberger, R. D. Dewhurst, M. Dietz, J. O. C. Jiménez-Halla, A. Trumpp, S. R. Wang, C. Brunecker, A. Haefner, A. Gärtner, T. Thiess, J. Böhnke, K. Radacki, R. Bertermann, T. B. Marder and H. Braunschweig, *J. Am. Chem. Soc.*, 2018, **140**, 13056–13063.
- 33 N. Arnold, H. Braunschweig, A. Damme, R. D. Dewhurst, L. Pentecost, K. Radacki, S. Stellwag-Konertz, T. Thiess, A. Trumpp and A. Vargas, *Chem. Commun.*, 2016, **52**, 4898–4901.
- 34 M. Arrowsmith, S. Endres, M. Heinz, V. Nestler, M. C. Holthausen and H. Braunschweig, *Chem.–Eur. J.*, 2021, **27**, 17660–17668.
- 35 A. Kerr, N. C. Norman, A. G. Orpen, M. J. Quayle, C. R. Rice, P. L. Timms, G. R. Whittell, A. Kerr and T. B. Marder, *Chem. Commun.*, 1998, 319–320.
- 36 N. Lu, N. C. Norman, A. Guy Orpen, M. J. Quayle, P. L. Timms and G. R. Whittell, *J. Chem. Soc., Dalton Trans.*, 2000, 4032–4037.
- 37 J. Bauer, H. Braunschweig, K. Kraft and K. Radacki, *Angew. Chem., Int. Ed.*, 2011, **50**, 10457–10460.
- 38 T. D. Quach, R. A. Batey and A. J. Lough, *Acta Crystallogr., Sect. E: Struct. Rep. Online*, 2001, **57**, o688–o689.
- 39 M. Mantina, A. C. Chamberlin, R. Valero, C. J. Cramer and D. G. Truhlar, *J. Phys. Chem. A*, 2009, **113**, 5806–5812.
- 40 W. Haubold, J. Herdtle, W. Gollinger and W. Einholz, *J. Organomet. Chem.*, 1986, **315**, 1–8.
- 41 W. Schacht and D. Kaufmann, *Chem. Ber.*, 1987, **120**, 1331–1338.
- 42 K. Samigullin, M. Bolte, H.-W. Lerner and M. Wagner, *Organometallics*, 2014, **33**, 3564–3569.
- 43 S. Griesbeck, Z. Zhang, M. Gutmann, T. Lühmann, R. M. Edkins, G. Clermont, A. N. Lazar, M. Haehnel, K. Edkins, A. Eichhorn, M. Blanchard-Desce, L. Meinel and T. B. Marder, *Chem.–Eur. J.*, 2016, **22**, 14701–14706.
- 44 K. Samigullin, Y. Soltani, H.-W. Lerner, M. Wagner and M. Bolte, *Acta Crystallogr., Sect. C: Struct. Chem.*, 2016, **72**, 189–197.
- 45 J. F. Blount, P. Finocchiaro, D. Gust and K. Mislow, *J. Am. Chem. Soc.*, 1973, **95**, 7019–7029.

